An Enhanced Navigation System for GPS Effectiveness

Rosen Miletiev[1], Emil Iontchev[2], Petar Kapanakov[3], Rumen Yordanov[4]
[1, 3, 4] Faculty of Telecommunications at Technical University of Sofia 8 Kl. Ohridski Blvd Sofia 1000, Bulgaria
{miletiev@tu-sofia.bg} {peshoteslata2@abv.bg} {rsyordanov@yahoo.com}

[2] Higher School of Transport "T.Kableshkov" 158 Geo Milev Street, Sofia 1574, Bulgaria
{e_iontchev@yahoo.com}

ABSTRACT: *The vehicular navigation systems largely depend on GPS models. The major limitations of GPS receivers towards the course estimation are recognized as a low update rate (up to 10 Hz) and the impossibility to provide continuous navigation solutions in the periods of no signal reception. In this paper we have developed a model for the course estimation from GNSS and IMU systems and analysis of the IMU accuracy and behaviour during the dead reckoning situation. During experimentation we found that the IMU system accurately calculated the heading angle and found to be more effective.*

Keywords: GNSS, MEMS, Inertial Navigation

Received: 1 November 2020, Revised 4 February 2021, Accepted 16 February 2021

DOI: 10.6025/ijwa/2021/13/2/52-58

1. Introduction

The GPS has become the primary source of providing navigation information for most of the present vehicular navigation applications [1-4]. However, the main disadvantages of GPS receivers towards the course estimation are recognized as a low update rate (up to 10 Hz) and the impossibility to provide continuous navigation solutions in the periods of no signal reception. In the opposite - an INS is a self-contained positioning device that continuously measures three orthogonal linear accelerations and three angular rates to calculate the required position. However, the error of accelerometers will be double integrated and cause position error that accumulate with time [5-7]. Typical factors, which have influence on the inertial sensor accuracy may be described as follows – null offset (bias), temperature hysteresis, gyroscope sensitivity to the linear accelerations, sampling noise, non – orthogonal sensor axes, etc.

The integration of GNSS and inertial system is the key to calculate position problem adequate for the typical automobile application where GPS is the primary navigation system, and dead reckoning is only needed to fill gaps in GPS coverage when buildings or terrain block the satellite signals [8-10].

2. System Description

The MEMS based inertial and navigation system is built to measure the linear and angular accelerations and to calculate the position while the integrated GPS receiver is used as a reference only with a refresh rate up to 10Hz. The block diagram of the proposed system is shown in Figure 1. The system is recognized as 9DoF (Degrees of Freedom) and it is based on 3D linear accelerometer, 3D digital gyroscope and 3D digital magnetometer (Figure 2). The inertial system uses MEMS three axes digital output linear accelerometer and magnetometer LSM303DLHC and 3D ultra-stable MEMS angular rate accelerometer L3G4200D, both produced by *ST*. The system reads the inertial and magnetic data 100 times per second and stores the navigation and inertial data in the internal FLASH memory (SD card) with a capacity up to 4GB. The GNSS system is based on the FTX GPS/GNSS antenna module type UC530M which has built-in multi-GNSS engine for combined GPS, GLONASS and QZSS, embedded GPS/GNSS antenna and extremely small form factor (9.6 x 14 x 1.95 mm) and low power consumption. The UC530M provides complete signal processing from embedded antenna to host port UART and location data output is in NMEA protocol. By utilizing GPS and GLONASS satellites in parallel, the GNSS module may enhance the position availability in harsh GNSS satellite visibility conditions.

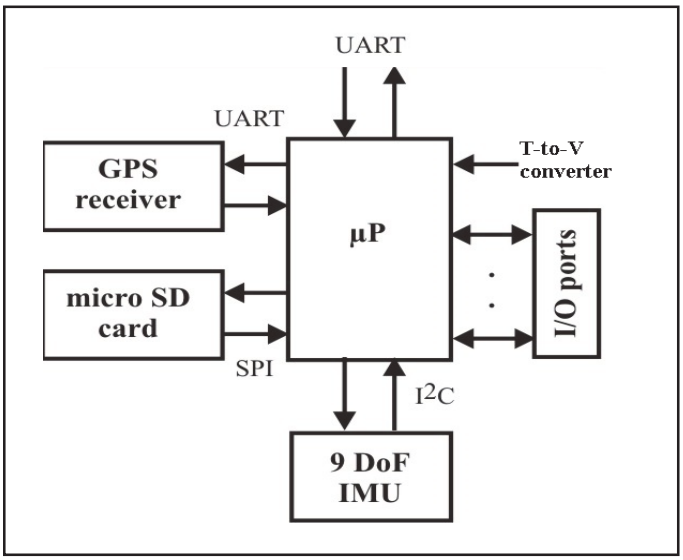

Figure 1. Block diagram of the proposed system

The inertial data are read by the navigation processor, which use an EKF to calculate pitch and roll angles (Figure 2) according to Eq. (2). The linear acceleration double integration process (Eqs. (3) and (4)) estimates the speed and the travelled distance.

The obtained results are used in the tilt-compensated compass to calculate the yaw angle. In the same time the gyroscope angular accelerations ω_x, ω_y, ω_z are numerically integrated using trapezoidal rule to calculate the yaw angle (heading) of the moving object according to the equations [11]:

$$\begin{aligned}
\varphi_x(i) &= \varphi_x(i-1) + \frac{\omega_x(i) + \omega_x(i-1)}{2}\Delta t \\
\varphi_y(i) &= \varphi_y(i-1) + \frac{\omega_y(i) + \omega_y(i-1)}{2}\Delta t \\
\varphi_z(i) &= \varphi_z(i-1) + \frac{\omega_z(i) + \omega_z(i-1)}{2}\Delta t
\end{aligned} \tag{1}$$

The tilt-compensated compass calculated the heading angle using magnetometer data *Mx*, *My, Mz* according to the equations [12]:

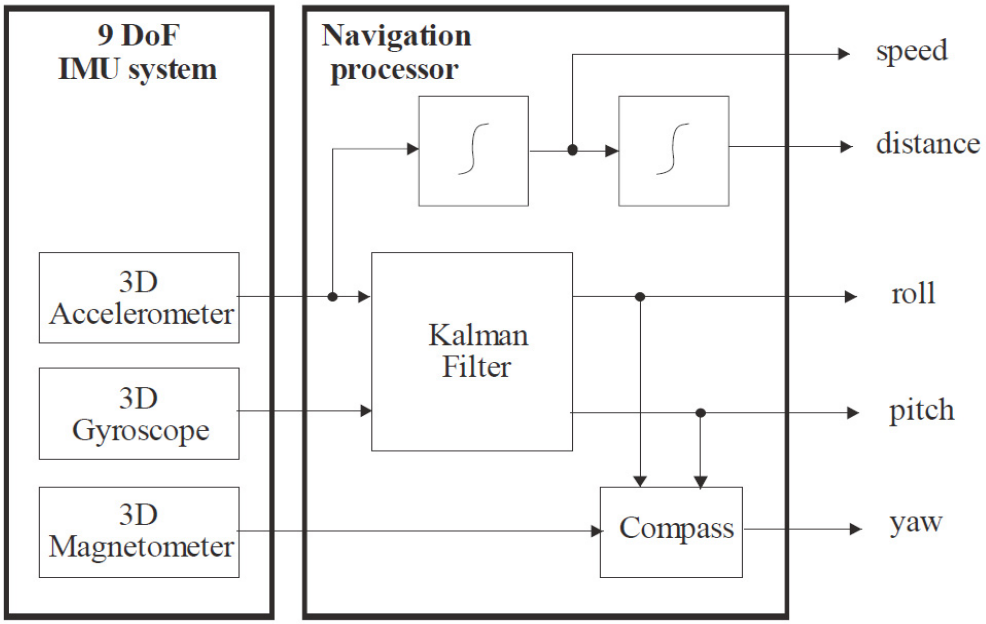

Figure 2. Proposed signal processing algorithm

$$
\begin{aligned}
X_H &= M_X \cos\phi + M_Y \sin\phi \sin\theta - M_Z \cos\theta \sin\phi \\
Y_H &= M_Y \cos\theta + M_Z \sin\theta \\
\varphi_0 &= arctg\left(\frac{Y_H}{M_H}\right) \\
\varphi &= \varphi_0 + \varphi_{declination}
\end{aligned}
\qquad (2)
$$

where $\phi - pitch, \theta - roll$ angles.

The declination angle $\varphi_{declination}$ for Sofia (Bulgaria) is equal to + $4^0 20'$ [13]. The 3D magnetometer is also preliminary calibrated towards soft-iron and iron-iron effects according to the algorithm described at [14].

In the same time the accelerometer data are numerically integrated using trapezoidal rule to calculate the speed *v* and travelled distance *d* of the moving object according to the equations [11]:

$$v_c(i) = v_c(i-1) + \frac{a(i) + a(i-1)}{2}\Delta t \qquad (3)$$

$$d_c(i) = d_c(i-1) + \frac{v_c(i) + v_c(i-1)}{2}\Delta t \qquad (4)$$

3. Experimental Results

The proposed system is tested on the road and the data are recorded on MMC/SD card and processed by MATLAB routine later. The system is placed between the front seats near the vehicle mass center and the IMU axes are orientated towards the vehicle axes according to Figure 3.

The sampling frequency of the inertial data is limited to 200Hz due to the limited time to send data to PC via RS232 interface. The test results are accomplished using lower sampling frequency which is equal to 20Hz. This sampling frequency is also chosen because the inertial blocks from 40 frames are stored in the single block of MMC/SD card and the

sampling frequency have to be multiple to 40Hz. Meanwhile the update rate of the GPS data is equal to 1Hz but it may be increased up to 10Hz in such matter that the IMU update ratio towards the GPS update ratio remains equal to 20.

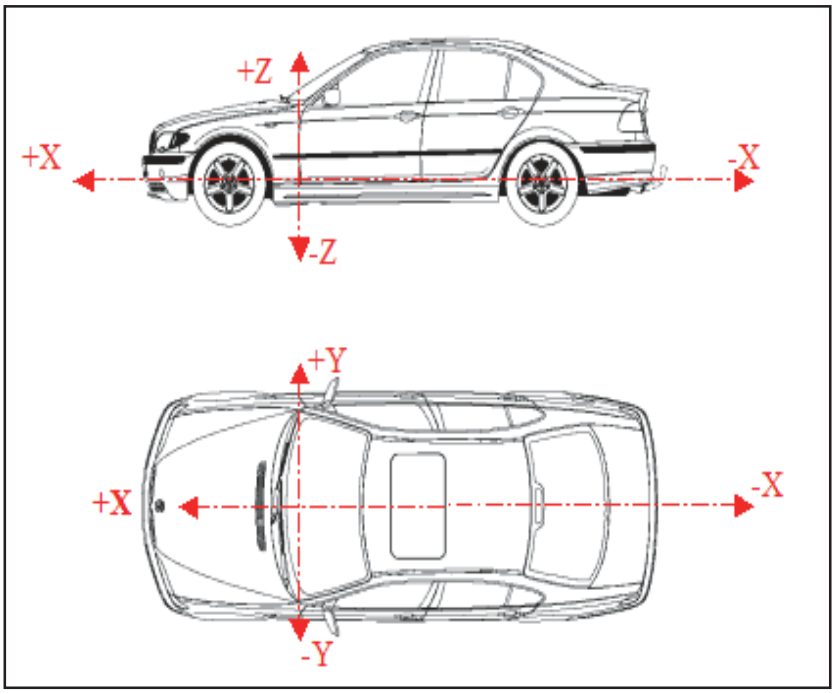

Figure 3. System orientation

The system is tested to record the navigation and the inertial data during some hours and the track is shown in Figure 4. It is clearly visible that the track is continuous except of the marked region with the red color. This region is extracted from the whole track and is shown below. There are three place named A, B and C where the track is interrupted which corresponded to the three tunnels (see the right map) due to the GPS signal lost.

This interruption is also clearly visible on the speed and course over ground shown in Figures 5 and 6 respectively.

Therefore the task of the inertial system is to restore the interrupted track and to ensure the course and the speed of the vehicle when the GPS signal is weak or lost. The restoration of the data is based on the calculation of the heading angle according to the signal processing algorithm (Figure 2). The calculated pitch and roll angles from the Kalman filter are used for the yaw angle estimation (heading angle). Simultaneously the speed and the travelled distance are also estimated by the navigation processor using a numerical integration of the accelerations (according to Eq. (3)) and speed (Eq. (4)) respectively.

The course is calculated in two ways and compared with the known COG data when GPS coverage is still active – the first value is obtained by the numerical integration of the angular rate gyroscope on the Z axis according to Eq. (1) and the second value is calculated by the e-compass according to Eq. (2). The results are shown in Figure 7.

The results show that both systems (gyroscope and magnetometer) correctly calculate the heading angle before entering into the first tunnel (approximately 150s from the track beginning). As the GPS signal is lost the gyroscope and the magnetometer continuously estimate the car course and when the GPS signal is restored the calculated heading angle from both systems is equal to the course of ground value from GNSS. The same situation appears when the car entered in the second tunnel but the estimated heading angle from the magnetometer is distorted probably by the steel elements in the tunnel structure. In a short period of time after beginning (approximately 400s) the gyroscope heading value starts to decline from the real value due to the uncompensated gyroscope bias accumulation. Therefore the gyroscope offset has to be compensated after the GPS signal restoration.

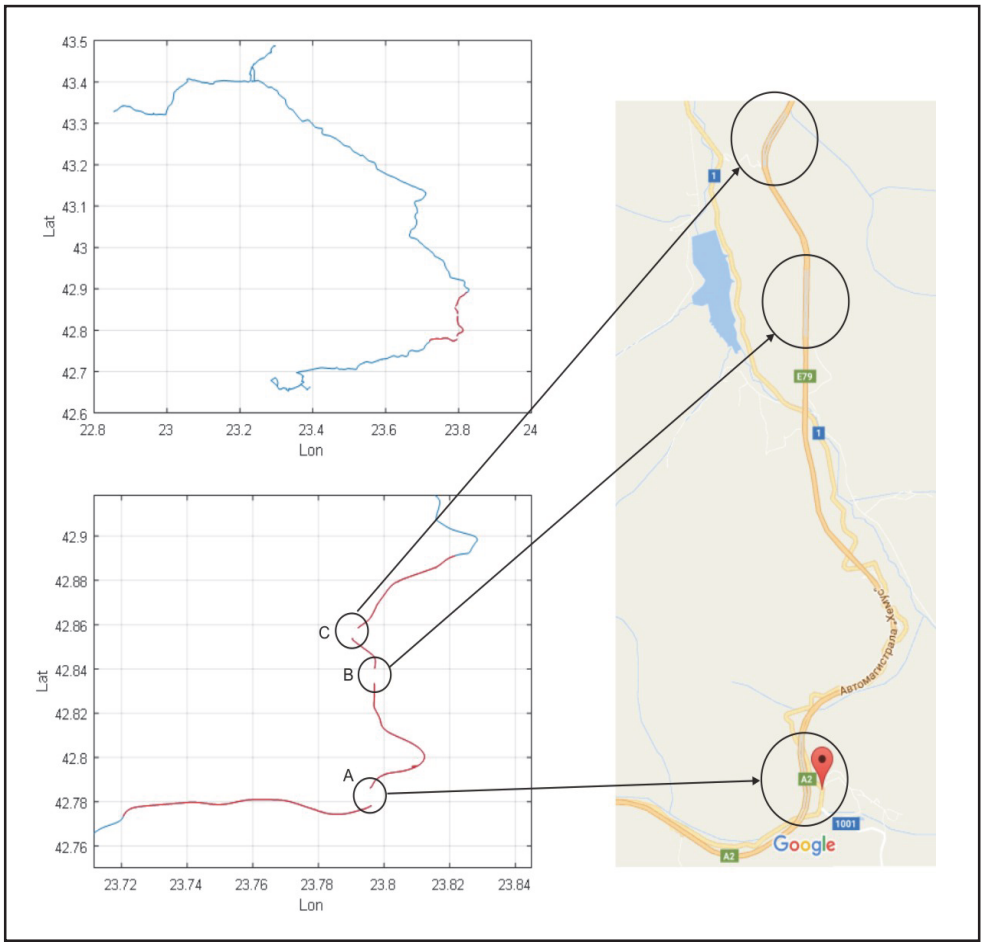

Figure 4. Track representation

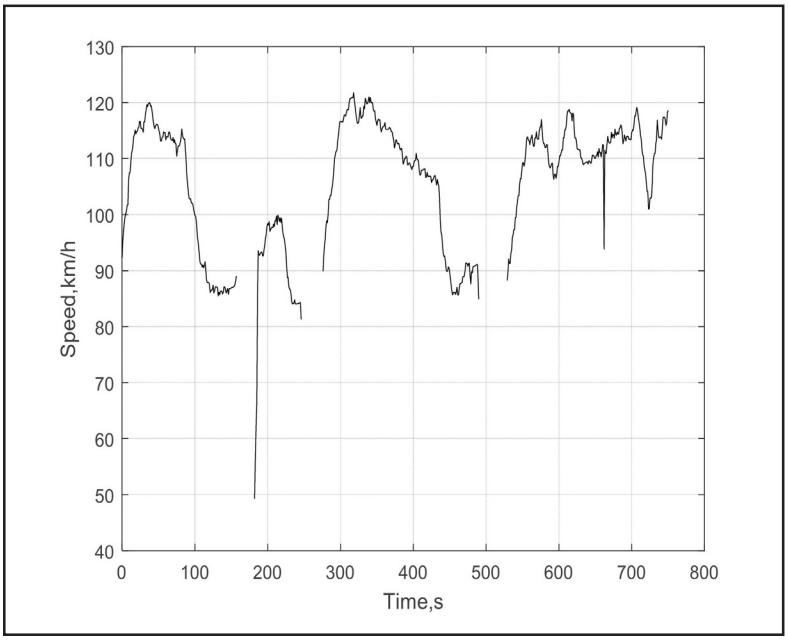

Figure 5. Recorded speed over ground (SOG)

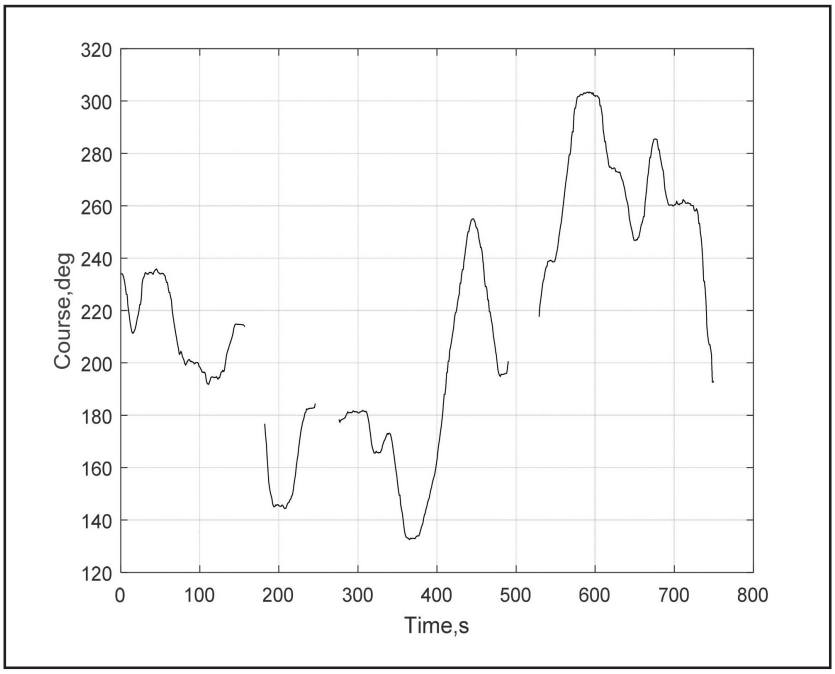

Figure 6. Recorder course over ground (COG)

The course is calculated in two ways and compared with the known COG data when GPS coverage is still active – the first value is obtained by the numerical integration of the angular rate gyroscope on the Z axis according to Eq. (1) and the second value is calculated by the e-compass according to Eq. (2). The results are shown in Figure 7.

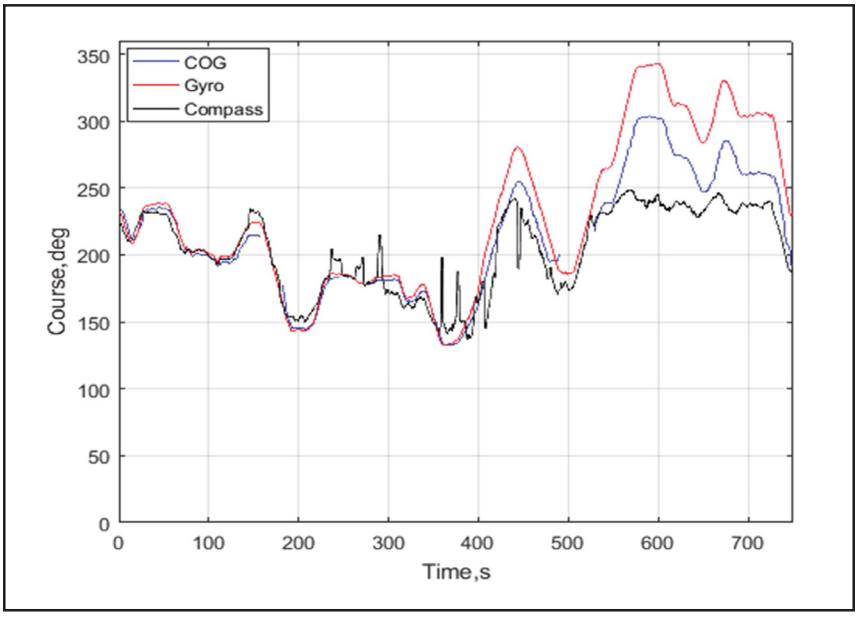

Figure 7. Heading angle estimation

The results show that both systems (gyroscope and magnetometer) correctly calculate the heading angle before entering into the first tunnel (approximately 150s from the track beginning). As the GPS signal is lost the gyroscope and the magnetometer continuously estimate the car course and when the GPS signal is restored the calculated heading angle from both systems is equal to the course of ground value from GNSS. The same situation appears when the car entered in the second

tunnel but the estimated heading angle from the magnetometer is distorted probably by the steel elements in the tunnel structure. In a short period of time after beginning (approximately 400s) the gyroscope heading value starts to decline from the real value due to the uncompensated gyroscope bias accumulation. Therefore the gyroscope offset has to be compensated after the GPS signal restoration.

4. Conclusion

The proposed system is tested towards the course estimation from GNSS and IMU systems and analysis of the IMU accuracy and behavior during the dead reckoning situation. It is shown that IMU system may accurately calculate the heading angle in two ways – numerical integration of the Z gyroscope data and Kalman filter implementation for the magnetometer data for a limited period of time. In the same time the angle estimation may be distorted by the numerical integration errors for the gyroscope or soft-iron effects for the magnetometer.

The future work will investigate the system capabilities towards reduction of the numerical integration errors by increasing the sampling frequency of the IMU system up to 200Hz. It is known that this error depends from the third degree of the sampling intervals so this error may be reduced significantly.

The IMU system may be used for inertial navigation based on the EKF due to the high sampling frequency and small integration errors, gaming, motion control, gyro stabilized platforms, MVEDR (Motor Vehicle Event Data Recorder) systems or crash monitor for aircrafts, trains or cars.

References

[1] Parkins, B.W., Spilker, J.J., Eds. (1996). *Global Positioning System: Theory and Applications*, Washington, DC: Amer. Inst. *Aeronautics Astronautics*, 1996, vol. II.

[2] Misra, P., Burke, B. P., Pratt, M. M. (1999). GPS Performance in Navigation, *Proceedings of the IEEE*, 87 (1) 65-85, (January).

[3] Hein, G. W. (2000). *From GPS and GLONASS via EGNOS to Galileopositioning and Navigation in the Third Millennium*, in *GPS Solutions*, 3 (4) 39-47, (April).

[4] Huang, J., Tan, H-S. (2006). A Low-order DGPS-based Vehicle Positioning System Under Urban Enviroment, *IEEE/ASME Trans. Mechatronics*, 5 (1-2) 567-575, (October).

[5] Caruso, M. J. (2000). *Applications of Magnetic Sensors for Low Cost Compass Systems*, PLANS, London 2000, p. 177.

[6] Electronic Tilt Compensation. Application Note AN-00MM- 004, Memsic 2008.

[7] Talat Ozyagcilar - Implementing a Tilt-Compensated eCompass using Accelerometer and Magnetometer Sensors, Freescale Semiconductor, Document Number: AN4248, Rev.3, 01/2012.

[8] Mohammed, A. Kh., Mokhtar, R. A., Eltahir, H. A. E. (2015). Target Coordinates Calculation using GPS/inertial-aided Sensors, 2015 International Conference on Computing, Control, Networking, Electronics and Embedded Systems Engineering *(ICCNEEE)*, 7-9 (September).

[9] Rogers, R. M. (2000). *Applied Mathematics in Integrated Navigation Systems*, American Institute of Aeronautics and Astonautics, Inc.

[10] Shin, E.-H. (2001). *Accuracy Improvement of Low Cost INS/GPS for Land Applications*, MA thesis University of Calgary, Calgary.

[11] Arraigada, M., Partl, M. (2006). Calculation of Displacements of Measured Accelerations, Analysis of Two Accelerometers and Application in Road Engineering, *6th Swiss Transport Research Conference*, Monte Verità/Ascona, March 15-17, 2006.

[12] Valenti, C. (2005). Microchip Technology Inc.AN996, Designing a Digital Compass Using the PIC18F2520 Microcontroller.

[13] http://magnetic-declination.com/.

[14] Stork, T. (2000). Philips Semiconductors, AN00022 - Electronic Compass Design using KMZ51 and KMZ52.